

A Ka-Band Geophysical Model Function

Alexey Nekrasov^{1,2,3}, Dmitry Popov⁴, Klaus Schünemann³

Abstract – A Ka-band geophysical model function is proposed. The model function is based on a similar previously-developed backscatter model, which showed a disadvantage at near cross-wind azimuths for incidence angles of 47° to 50°. The new Ka-band geophysical model function is valid for incidence angles of 30° to 50° at vertical transmit and receive polarization. Several particular cases of water-surface backscattering are presented by using this function.

Keywords – Scatterometer, Geophysical model function, Ka-Band, Sea Wind.

I. INTRODUCTION

Many researchers have been investigating the microwave backscattering signatures of the water surface and solving the problem of remotely measuring wind over water during the last decades. A typical method for describing sea clutter is in the form of the normalized radar cross section (NRCS), the statistical distribution of the NRCS, the amplitude correlation and the spectral shape of the Doppler returns [1].

Use of a scatterometer, radar designed for measuring the surface scattering characteristics allows for studying sea surface backscattering and to estimate the wind vector over water because the NRCS of the water surface depends on wind speed and direction. Based on experimental data and scattering theory, a significant number of empirical and theoretical backscatter models and algorithms for retrieval of near-surface wind vector over water from satellite and airplane have been proposed [2–14]. This field develops actively with improvements of current and appearance of new models [15–22].

The backscatter of radio waves from sea surface varies considerably according to the incidence angle [6]. Near nadir, there is a region of quasi-specular return with a maximum of NRCS that decreases when increasing the angle of incidence. Between incidence angles of about 20° and 70°, the NRCS falls smoothly in a so-called “plateau” region. For medium incidence angles, microwave radar backscatter is predominantly due to the presence of capillary-gravity wavelets, which are superimposed on large gravity waves of the sea surface.

Article history: Received April 17, 2016; Accepted July 06, 2017

^{1,2,3}Alexey Nekrasov is with Saint Petersburg Electrotechnical University, Popova 5, 197376 Saint Petersburg, Russia; with the Southern Federal University, Chekhova 2, 347922 Taganrog, Rostov Region, Russia; and with Hamburg University of Technology, Denickestraße 22, 21073 Hamburg, Germany, E-mail: alexei-nekrassov@mail.ru

⁴Dmitry Popov is with Moscow Polytechnic University, Bolshaya Semenovskaya 38, 107023 Moscow, Russia, E-mail: damitry@mail.ru

³Klaus Schünemann is with Hamburg University of Technology, Denickestraße 22, 21073 Hamburg, Germany, E-mail: schuenemann@tu-harburg.de

Small-scale sea waves of a length of approximately one half the radar wavelength are in Bragg resonance with an incident electromagnetic wave. At incidence angles greater than about 70°, there is a “shadow” region in which the NRCS falls dramatically, due to the shadowing effect of waves which are close to the radar blocking waves farther away.

The wind blowing over the sea modifies the water-surface backscatter properties. These depend on both wind speed and direction. The wind speed U can be determined by a scatterometer because a stronger wind will produce a larger NRCS $\sigma^\circ(U, \theta, \alpha)$ at a medium incidence angle θ , and a smaller NRCS at a small (near nadir) incidence angle. Wind direction can also be inferred because the NRCS varies as a function of the azimuth angle α relative to the up-wind direction [12].

To retrieve the wind vector from NRCS measurements, the relationship between NRCS and near-surface wind, called the “geophysical model function”, must be known. Scatterometer experiments have shown that the NRCS model function for medium incidence angles at appropriate transmit and receive polarization (vertical or horizontal) can be presented in several various forms. One of the widely used forms for the geophysical model function is [12]

$$\sigma^\circ(U, \theta, \alpha) = A(U, \theta) + B(U, \theta) \cdot \cos \alpha + C(U, \theta) \cdot \cos(2\alpha), \quad (1)$$

where $A(U, \theta)$, $B(U, \theta)$ and $C(U, \theta)$ are the Fourier terms that depend on sea surface wind speed and incidence angle, $A(U, \theta) = a_0(\theta) \cdot U^{\gamma_0(\theta)}$, $B(U, \theta) = a_1(\theta) \cdot U^{\gamma_1(\theta)}$, and $C(U, \theta) = a_2(\theta) \cdot U^{\gamma_2(\theta)}$; $a_0(\theta)$, $a_1(\theta)$, $a_2(\theta)$, $\gamma_0(\theta)$, $\gamma_1(\theta)$ and $\gamma_2(\theta)$ are the coefficients depending on the incidence angle. The term $A(U, \theta)$ equals the azimuthally averaged NRCS; the term $B(U, \theta)$ embodies the upwind-downwind asymmetry; and the term $C(U, \theta)$ represents the upwind-crosswind anisotropy. Detailed procedures to obtain the above terms from backscatter values in the up-wind, down-wind, and cross-wind directions have been reported in [23]. The coefficients $a_0(\theta)$, $a_1(\theta)$, $a_2(\theta)$, $\gamma_0(\theta)$, $\gamma_1(\theta)$ and $\gamma_2(\theta)$ are determined empirically for an appropriate geophysical model function by using airborne or satellite measurements and validating surface measurements in addition. The coefficients are tabulated or presented as functions of incidence angle [2, 5, 8, 24].

Technological progress has made it possible to use a Ka-band technique for airborne and satellite remote sensing. The usage of such a high frequency allows for reduced dimensions of the instruments on board as well as for increased resolution and accuracy in the estimation of sea surface topography [25].

Thus, there is a growing interest in studying Ka-band water surface backscattering and in developing the geophysical

model function for this band. The Ka-band backscatter from water surface has been studied by using NRCS data from several airborne and wind-wave tank scatterometer experiments [4, 15, 25–29].

In this connection, an improved Ka-band geophysical model function will be presented below.

II. GEOPHYSICAL MODEL FUNCTION

A Ka-band geophysical model function of the form (1) for incidence angles of 30° to 50° at vertical transmit and receive polarization has been previously presented in [28]. That geophysical model function has been developed using another NRCS model function from [4] given, however, only for up-, down- and cross-wind directions. Under the model development, the original up-wind NRCS curve from [4] at an incidence angle of 30° has been corrected in accordance with the wind-wave tank results reported in [23]. The correction had to be done, because the down-wind NRCS values tended to exceed the up-wind NRCS values at lower wind speeds as well as the down-wind NRCS values tended to exceed the cross-wind NRCS values at higher wind speeds.

Unfortunately, the geophysical model function described in [28] has a disadvantage. It shows up as a trough with a subsequent increase of the curve at incidence angles of 47° to 50° for near cross-wind azimuths, especially at low wind speeds.

To eliminate this imperfection, the model of the form (1) given in [28] has been recalculated. The following new coefficients for the Ka-band geophysical model function for vertical transmit and receive polarization, incidence angles of 30° to 50° and wind speeds of 5 to 20 m/s have been obtained

$$\begin{aligned}
 a_0(\theta) &= 0.006036 - 0.0002031 \cdot \theta + 0.00000168 \cdot \theta^2, \\
 a_1(\theta) &= -0.007776 + 0.0004421 \cdot \theta - 0.000005692 \cdot \theta^2, \\
 a_2(\theta) &= 0.001151 + 0.0000134 \cdot \theta - 0.000000689 \cdot \theta^2, \\
 \gamma_0(\theta) &= 4.902 - 0.198 \cdot \theta + 0.0028 \cdot \theta^2, \\
 \gamma_1(\theta) &= 13.618 - 0.631 \cdot \theta + 0.00753 \cdot \theta^2, \\
 \gamma_2(\theta) &= 5.896 - 0.258 \cdot \theta + 0.00348 \cdot \theta^2, \quad (2)
 \end{aligned}$$

where θ is the incidence angle in degrees.

Figs. 1-3 show NRCS curves of form (1) with coefficients (2) versus incidence angle at wind speeds of 5, 10, 15, and 20 m/s for azimuth angles of 70° , 90° , and 110° , respectively, at vertical transmit and receive polarization. Fig. 4 gives an example of NRCS curves versus azimuth angle for incidence angle of 40° at wind speeds of 5, 10, 15, and 20 m/s, respectively.

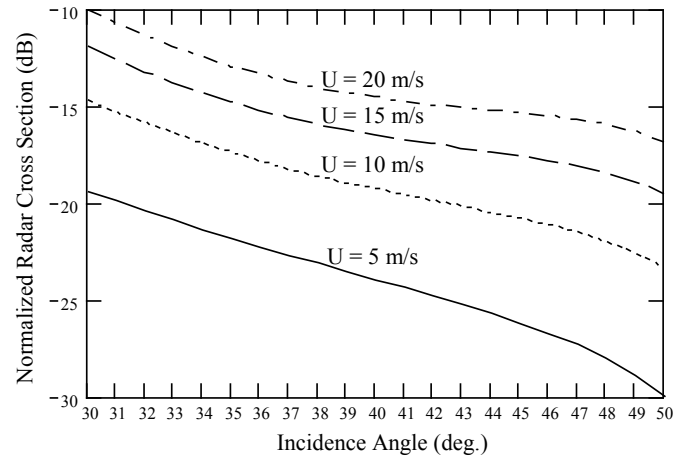


Fig. 1. Ka-band NRCS versus incidence angle for azimuth angle of 70° at wind speeds of 5, 10, 15, and 20 m/s, respectively, at vertical transmit and receive polarization

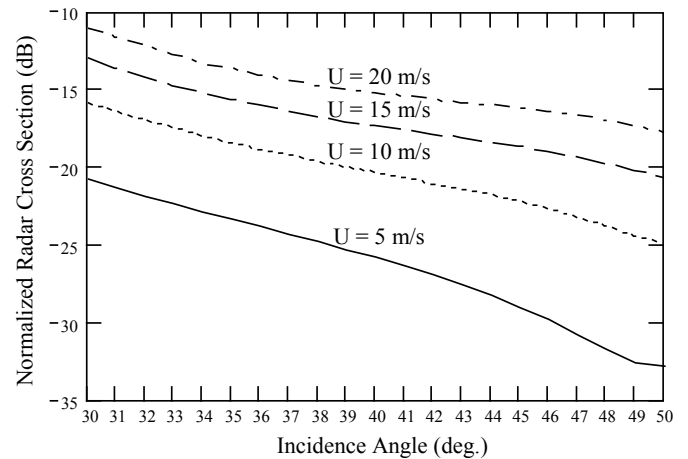


Fig. 2. Ka-band NRCS versus incidence angle for azimuth angle of 90° at wind speeds of 5, 10, 15, and 20 m/s, respectively, at vertical transmit and receive polarization

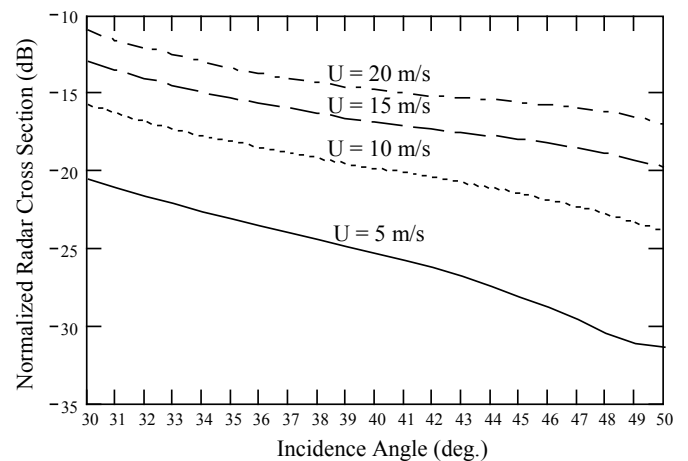


Fig. 3. Ka-band NRCS versus incidence angle for azimuth angle of 110° at wind speeds of 5, 10, 15, and 20 m/s, respectively, at vertical transmit and receive polarization

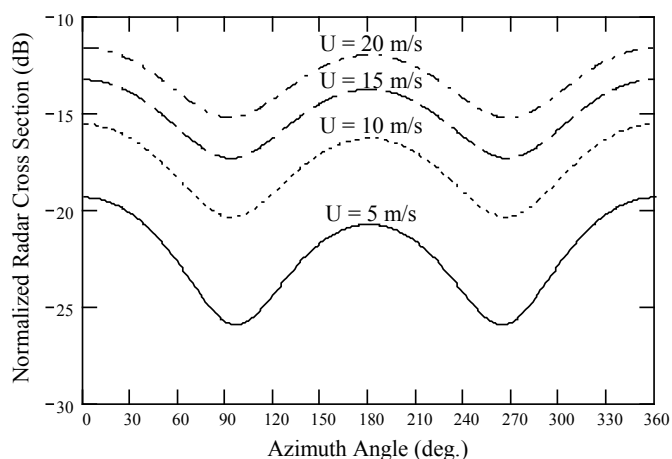


Fig. 4. Ka-band NRCS versus azimuth angle for incidence angle of 40° at wind speeds of 5, 10, 15, and 20 m/s, respectively, at vertical transmit and receive polarization

Thus, the new coefficients obtained for the geophysical model function of form (1) have allowed to eliminate the disadvantage of the previously-developed backscatter model.

III. CONCLUSION

The previously-developed Ka-band backscatter model for incidence angles of 30° to 50° at vertical transmit and receive polarization [28] has been improved by eliminating its disadvantage near to cross-wind azimuths at incidence angles of 47° to 50° .

The improved geophysical model function can be used for developing and testing the wind retrieval algorithms for Ka-band remote sensing instruments.

ACKNOWLEDGEMENT

We would like to acknowledge the financial support of this work by the Russian Science Foundation (project No. 16-19-00172). The authors would also like to express their sincere thanks to Hamburg University of Technology for the research opportunities provided. A.N. would like to thank the German Academic Exchange Service (DAAD) for an exchange visit support.

REFERENCES

- [1] D. G. Money, A. Mabogunje, D. Webb, and M. Hooker, "Sea Clutter Power Spectral Lineshape Measurements", *Radar'97*, Edinburgh, UK, 1997, pp. 85-89.
- [2] R. K. Moore, and A. K. Fung, "Radar Determination of Winds at Sea", *Proc. IEEE*, vol. 67, no. 11, pp. 1504-1521, Nov. 1979.
- [3] D. B. Chelton, and P. J. McCabe, "A Review of Satellite Altimeter Measurement of Sea Surface Wind Speed: With a Proposed New Algorithm", *J. Geophys. Res.*, vol. 90, no. C3, pp. 4707-4720, May 1985.
- [4] H. Masuko, K. Okamoto, M. Shimada, and S. Niwa, "Measurement of Microwave Backscattering Signatures of the Ocean Surface Using X Band and Ka Band Airborne Scatterometers", *J. Geophys. Res.*, vol. 91, no. C11, pp. 13065-13083, Nov. 1986.
- [5] V. Wismann, *Messung der Windgeschwindigkeit über dem Meer mit einem flugzeuggetragenen 5.3 GHz Scatterometer*, Dissertation zur Erlangung des Grades eines Doktors der Naturwissenschaften, Bremen, Germany: Universität Bremen, 119 S., 1989.
- [6] P. H. Hildebrand, "Estimation of Sea-surface Wind Using Backscatter Cross-section Measurements from Airborne Research Weather Radar", *IEEE Trans. Geosci. Remote Sens.*, vol. 32, no. 1, pp. 110-117, Jan. 1994.
- [7] J. R. Carswell, S. C. Carson, R. E. McIntosh, F. K. Li, G. Neumann, D. J. McLaughlin, J. C. Wilkerson, P. G. Black, and S. V. Nghiem, "Airborne Scatterometers: Investigating Ocean Backscatter Under Low- and High-wind Conditions", *Proc. IEEE*, vol. 82, no. 12, pp. 1835-1860, Dec. 1994.
- [8] D. G. Long, M. A. Donelan, M. H. Freilich, H. C. Graber, H. Masuko, W. J. Pierson, W. J. Plant, D. Weissman, and F. Wentz, *Current Progress in Ku-band Model Functions*, Tech. Rep. MERS 96-002, Brigham Young University, USA, pp. 88, 1996.
- [9] F. J. Wentz, S. Peteherych, and L. A. Thomas, "A Model Function for Ocean Radar Cross Sections at 14.6 GHz", *J. Geophys. Res.*, vol. 89, no. C5, pp. 3689-3704, Sep. 1984.
- [10] I. R. Young, "An Estimate of the Geosat Altimeter Wind Speed Algorithm at High Wind Speeds", *J. Geophys. Res.*, vol. 98, no. C11, pp. 20275-20285, Nov. 1993.
- [11] R. Romeiser, A. Schmidt, and W. Alpers, "A Three-scale Composite Surface Model for the Ocean Wave-radar Modulation Transfer Function", *J. Geophys. Res.*, vol. 99, no. C5, pp. 9785-9801, May 1994.
- [12] M. W. Spencer, and J. E. Graf, "The NASA Scatterometer (NSCAT) Mission", *Backscatter*, vol. 8, no. 4, pp. 18-24, Nov. 1997.
- [13] O. Isoguchi, and M. Shimada, "An L-band Ocean Geophysical Model Function Derived from PALSAR", *IEEE Trans. Geosci. Remote Sens.*, vol. 47, no. 7, pp. 1925-1936, Jul. 2009.
- [14] F. Nirchio, and S. Venafrà, "XMOD2 – An Improved Geophysical Model Function to Retrieve Sea Surface Wind Fields from Cosmo-SkyMed X-band Data", *Eur. J. Remote Sens.*, vol. 46, pp. 583-595, 2013.
- [15] R. M. Gairola, M. T. Bushair, and S. A. Bhowmick MSc, "Geophysical Model Function for Wind Speed Retrieval from SARAL-Altika", *Mar. Geod.*, vol. 38, supp. 1, 26 p., Apr. 2015, doi: 10.1080/01490419.2015.1036182.
- [16] L. Ricciardulli, and F. Wentz, "Progress and Future Plans on an Ocean Vector Wind Climate Record", *IOVWST Meeting Presentation*, Brest, France, Jun. 2014, https://coaps.fsu.edu/scatterometry/meeting/docs/2014/ClimateDataRecord/Ricciardulli_ovwst_2014_CDR_posted.pdf.
- [17] Y. Takeyama, T. Ohsawa, K. Kozai, C. B. Hasager, and M. Badger, "Comparison of Geophysical Model Functions for SAR Wind Speed Retrieval in Japanese Coastal Waters", *Remote Sens.*, vol. 5, no. 4, pp. 1956-1973, Apr. 2013.
- [18] S. H. Yueh, W. Tang, A. G. Fore, G. Neumann, A. Hayashi, A. Freedman, J. Chaubell, and G. S.E. Lagerloef, "L-Band Passive and Active Microwave Geophysical Model Functions of Ocean Surface Winds and Applications to Aquarius Retrieval", *IEEE Trans. Geosci. Remote Sens.*, vol. 51, no. 9, pp. 4619-4632, Sep. 2013.
- [19] F. Fois, P. Hoogeboom, F. Le Chevalier, and A. Stoffelen, "Future Ocean Scatterometry: On the Use of Cross-polar Scattering to Observe Very High Winds", *IEEE Trans. Geosci. Remote Sens.*, vol. 53, no. 9, pp. 5009-5020, Apr. 2015.
- [20] Y. Y. Yurovsky, V. N. Kudryavtsev, S. A. Grodsky, and B. Chapron, "Ka-Band Dual Copolarized Empirical Model for the Sea Surface Radar Cross Section", *IEEE Trans. Geosci. Remote Sens.*, vol. 55, no. 3, pp. 143-148, Mar. 2017.

- [21] Y. Y. Yurovsky, V. N. Kudryavstev, S.A. Grodsky, and B. Chapron, "Sea Surface Radar Backscattering Cross-section in Ka-band," *37th Asian Conference on Remote Sensing ACRS 2016*, Colombo, Sri Lanka, 2016, vol. 3, pp. 1924-1932.
- [22] A. Wineteer, B. Stiles, and E. Rodriguez, "DopplerScatt Wind Retrieval", *International Ocean Vector Winds Science Team Meeting Presentation*, San Diego, California, May 2017, https://mdc.coaps.fsu.edu/scatterometry/meeting/docs/2017/docs/Tuesday/morning/SecondSession/1053_wineteer_ds_winds_ovvst2017_v3.pdf.
- [23] S. V. Nghiem, F. K. Li, and G. Neumann, "The Dependence of Ocean Backscatter at K_u -band on Oceanic and Atmospheric Parameters", *IEEE Trans. Geosci. Remote Sens.*, vol. 35, no. 3, pp. 581-600, May 1997.
- [24] A. Bentamy, S. A. Grodsky, J. A. Carton, D. Croizé-Fillon, and B. Chapron, "Matching ASCAT and QuikSCAT Winds," *J. Geophys. Res.*, vol. 117, no. C02011, pp. 1-15, Feb. 2012, doi:10.1029/2011JC007479.
- [25] O. Boisot, S. Pioch, C. Fatras, G. Caulliez, A. Bringer, P. Borderies, J.-C. Lalaurie, and C.-A. Guérin, "Ka-band Backscattering from Water Surface at Small Incidence: A Wind-wave Tank Study", *J. Geophys. Res. Oceans*, vol. 120, no. 5, pp. 3261-3285, May 2015.
- [26] J.-P. Giovanangeli, L. F. Bliven, and O. L. Calve, "A Wind-Wave Tank Study of the Azimuthal Response of a Ka-band Scatterometer", *IEEE Trans. Geosci. Remote Sens.*, vol. 29, no. 1, pp. 143-148, Jan. 1991.
- [27] S. Tanelli, S. L. Durden, and E. Im, "Simultaneous Measurements of Ku- and Ka-band Sea Surface Cross Sections by an Airborne Radar", *IEEE Geosci. Remote Sens. Lett.*, vol. 3, no. 3, pp. 359-363, July 2006.
- [28] A. Nekrasov, and P. Hoogeboom, "A Ka-band Backscatter Model Function and an Algorithm for Measurement of the Wind Vector over the Sea Surface", *IEEE Geosci. Remote Sens. Lett.*, vol. 2, no. 1, pp. 23-27, Jan. 2005.
- [29] D. Mapelli, N. Pierdicca, L. Guerriero, P. Ferrazzoli, E. Calleja, B. Rommen, D. Giudici, and A. Monti Guarnieri, "A Comparative Study of Radar Ka-band Backscatter", *Proc. SPIE*, vol. 9243, SAR Image Analysis, Modeling, and Techniques XIV, 92430U, 13 p., Oct. 2014.